Modification and Characterization of Nano-Ag/TiO_2 Antimold Agent for Wood Materials

Lin Lin Yingni Yang Brian K. Via
Yi Liu Hongwu Guo Fan Zhang

Abstract

Nano-Ag/TiO_2 exhibits effective antimicrobial activities; however, its tendency to aggregate limits its application in wood products for improved antimold properties. In this study, nano-Ag/TiO_2 was modified by a silane coupling agent (γ-aminopropyltriethoxysilane [KH-550]) and then loaded into wood via vacuum impregnation. The effects of KH-550 concentration, Ag/TiO_2 concentration, reaction temperature, and incubation time on the antimold rate, loading amount, and leach resistance for wood materials were investigated. Results showed that the antimold rate, loading amount, and fixation rate of mold-proof–treated wood was strengthened by KH-550 modification. The binding affinity and surface energy of nano-Ag/TiO_2 was reduced, and the dispersivity of nano-Ag/TiO_2 particles was improved after modification. Observation by field emission scanning electron microscopy showed that the modified nano-Ag/TiO_2 penetrated into the wood tracheids and formed a tight flocculent structure. X-ray diffractive analysis confirmed that modification did not affect the anatase diffraction pattern of nano-Ag/TiO_2 or its photocatalytic and antimicrobial activities. Characterization by Fourier transform infrared spectroscopy showed that modified nano-Ag/TiO_2 efficiently cross-linked with wood hydroxyl groups. This work provided a simple and effective method to develop a novel nano-Ag/TiO_2 antimold agent for wood mold-proof treatment.

Wood is an ideal material for furniture manufacture, timber construction, and interior decoration (Liu et al. 2015a, 2015b). However, as a natural biomass material, wood is predisposed to mildew during use, especially after exposure to damp conditions. Mold growth not only negatively affects the physical and chemical properties but also shortens the service life, resulting in increased global consumption of forest resources. As a novel antimold agent, nano-TiO_2 has garnered increased research attention in recent years because of its stable chemical properties, high catalytic activity, low cost, and environmental friendliness.

TiO_2 is an n-type semiconductor catalyst. Under UV-light irradiation, its electron-hole pairs facilitate the formation of hydroxyl radicals and superoxide anions from O_2 and H_2O, which react with the cell wall, plasma membrane, or intracellular components of bacteria or fungus and thus kill the microbes or inhibit their growth (Rincón and Pulgarin 2004). Furthermore, the reactive oxygen species decompose bacterial endotoxins and completely break down bacteria remnants and the organic nutrients. In addition, TiO_2 is self-cleaning (Akira et al. 2000). However, the antimicrobial activities of nano-TiO_2 are significantly weakened when exposed to natural light, low light, or even worse, darkness (Feng et al. 2009), and this limits its practical application. One innovative method to mitigate these problems is to load nano-Ag onto TiO_2 before impregnation into wood. The shallow potential wells of Ag can capture photosensitive electrons and thus extend the lifetime of photosensitive carriers, resulting in enhanced catalytic activity of TiO_2. Further, nano-Ag particles exhibit favorable antimicrobial activity and perform synergistic bactericidal effects in tandem with TiO_2 (Rengaraj and Li 2006, Wang et al. 2015).

The authors are, respectively, Lecturer, MOE Key Lab. of Wooden Material Sci. and Application, Beijing Key Lab. of Wood Sci. and Engineering, and MOE Engineering Research Center of Forestry Biomass Materials and Bioenergy, Beijing Forestry Univ., Beijing, China, and Forestry College of Beihua Univ., Jilin, China (13381448456@163.com); Doctoral Master Student, MOE Key Lab. of Wooden Material Sci. and Application, Beijing Forestry Univ., Beijing, China (13121664993@163.com); Professor, Forest Products Development Center, School of Forestry and Wildlife Sci., Auburn Univ., Auburn, Alabama (bkv0003@auburn.edu); and Lecturer, Professor, and Professor, MOE Key Lab. of Wooden Material Sci. and Application, Beijing Forestry Univ., Beijing, China (liuyi.zhongguo@163.com [corresponding author], ghw5052@163.com [corresponding author], zhangfan1976@163.com). This paper was received for publication in February 2017. Article no. 17-00016.

Forest Prod. J. 68(1):70–77.
doi:10.13073/FPJ-D-17-00016

Nano-TiO_2–wood composites have been manufactured via direct dispersion, the sol-gel method, and hydrothermal methods to enhance the flame resistance, antimicrobial effects, superhydrophobicity, and antiaging properties of wood materials (Miyafuji and Saka 1997, Akira et al. 2000, Rincón and Pulgarin 2004, Ye 2006, Nelson and Deng 2008, Xue et al. 2008, Sun et al. 2010, Sun 2012, Wang 2012, Zhou 2015). Direct dispersion methods are widely used, and nano-TiO_2 in various forms is prepared and dissolved in solvents and loaded into wood by soaking it in the solution. The simplicity of this procedure makes it ideal for industrial applications; however, after addition of Ag, nano-TiO_2 presents strong polarity and tends to form large aggregates significantly undermining its functional efficiency. Thus, innovative schemes, such as efficient dispersants, surface modification, or ultrasonic dispersion, have been employed to prevent aggregation (Ye 2006, Wang 2012, Zhou 2015). Rengaraj and Li (2006) modified nano-TiO_2 using a silane coupling agent (γ-[2,3-epoxypropoxy] propytrimethoxysilane [KH-560]) and maleic anhydride as couplers. This modification reduced nano-TiO_2 aggregation and resulted in a smaller particle size of 30 to 80 nm. It is hypothesized that modification by silane couplers produces a monomolecular layer on nano-TiO_2 and thus significantly reduces the surface energy and the binding affinity of the TiO_2 particles. Wang (2012) improved the dispersion of the nano-TiO_2–wood preservative by adding titanate coupling agent (NDZ-105) and sodium hexametaphosphate surfactant. After modification, the weight gain and fixation rate of the wood preservative increased remarkably, suggesting that the surface modification of TiO_2 is able to improve wood rot–resistant properties. Zhou (2015) modified the nano-TiO_2 with KH-550 and applied melamine-formaldehyde resin containing the modified nano-TiO_2, and this system was used to bond wood veneers. It was found that the modified nano-TiO_2 addition increased the antibacterial ratio of the wood composites to 99 percent. Despite the recent literature, the effects of modified TiO_2 on antifungal performance of wood properties have not been explored.

In this study, a nano-Ag/TiO_2 was modified with the silane coupling agent (KH-550) and then loaded into wood via vacuum impregnation. The effects of KH-550 concentration, Ag/TiO_2 concentration, reaction temperature, and incubation time on the antimold rate, loading amount, and leach resistance of the resulting wood samples were investigated by multifactor experiment. Field emission scanning electron microscopy (FE-SEM), X-ray diffraction (XRD), and Fourier transform infrared spectroscopy (FTIR) were utilized to measure or understand the response variables. This work provided a simple and effective method to develop a novel nano-Ag/TiO_2 antimold agent for wood mold-proof treatment.

Materials and Methods

Materials

Masson pine wood (*Pinus massoniana* Lamb.) was purchased from Jilin Province, northeastern China. The air-dried sapwood of Masson pine was sawn and prepared into 20 by 5 by 50-mm-size specimens for antimold tests. Specimens for various loading conditions and leach resistance tests were cut into 20 by 20 by 20-mm sections. All specimens were sanded with 200-mesh sandpaper to ensure a smooth and flat surface, and all were free of mold, blue stain, insect boring marks, and knots. Nano-Ag/TiO_2 (anatase type, average size: 30 nm; mass fraction of silver: 1%) was purchased from Hangzhou Wanjing New Material Co. (Hangzhou, China). Silane coupling agent (KH-550) was obtained from Dinghai Plastic Chemical Co. (Dongguan, China), and ethyl alcohol (analytical grade) was obtained from Beijing Chemical Works (Beijing, China).

Nano-Ag/TiO_2 modification

KH-550 solution was prepared from 20 wt% silane coupling agent KH-550, 8 wt% deionized water, and 72 wt% ethanol. The pH value of the KH-550 solution was adjusted to 4 with acetic acid. Nano-Ag/TiO_2 ethanol dispersion (2.5, 5, 7.5, or 10 percent [wt/vol]) was prepared and stirred (1,000 rps) for 10 minutes, and then 0.5, 1, 1.5, or 2 percent (wt/vol) KH-550 solution was added, and the mixtures were stirred for another 10 minutes. After that, the mixtures were incubated at 20°C, 40°C, 60°C, and 80°C for 1, 2, 4, and 6 hours, respectively. Details of the experimental parameters are provided in Table 1. The mixtures were cooled to room temperature and then centrifuged at 5,000 rpm for 10 minutes. The precipitated modified nano-Ag/TiO_2 was dispersed via ultrasonic dispersion (40 KHz, 300 W) in ethanol; the centrifuge treatment was repeated three times, and finally a modified water-soluble nano-Ag/TiO_2 was obtained.

Vacuum impregnation

The modified water-soluble nano-Ag/TiO_2 was dissolved in ethanol at 2.5, 5, 7.5, and 10 wt%. Masson pine wood specimens were soaked in the solution for 10 minutes under 0.02 MPa vacuum and then for 1 hour under atmospheric pressure at ambient temperature. After that, the specimens were dried in a vacuum oven, pulled out, and weighed.

Properties of antimold rate

The property tests of antimold rate were conducted in accordance with the Chinese standard GB/T 18261-2000 (China Timber Standardization Technical Committee 2000). Thirty wood specimens were treated with each specific condition shown in Table 1 and then soaked in deionized water for 48 hours to ensure that the specimens contained enough water for mold growth. All the specimens were incubated at ambient temperature with 90 percent humidity in an oven containing saturated KNO_3 solution for 30 days. Mold growth on the wood surface was observed carefully, and classifications were made. Specimens with no obvious mold or blue-stain fungi on the surface ($<5\%$ of total surface area), and those that showed no or only slight blue-stain fungi (<5 total area), were considered mold resistant. Antimold rate is normally expressed as the percentage of mold-resistant specimens.

Properties of loading amount

Six specimens were treated with each specific condition described in Table 1, respectively, and then dried in an oven at 40°C until reaching a constant weight. All of the specimens were weighed (m_1) and then soaked in the antimold preservative. Residual liquid on the specimens was removed by absorbent paper, and then the sample was weighed again (m_2). The loading amount (R) was calculated according to the equation

Table 1.—Process parameters for nano-Ag/TiO_2 modification.

No.	Concentration of KH-550 in ethyl alcohol (wt%)	Concentration of nano-Ag/TiO_2 (wt%)	Reaction temperature (°C)	Incubation time (h)
1	0, 0.5, 1, 1.5, 2	5	80	2
2	1	2.5, 5, 7.5, 10	80	2
3	1	5	20, 40, 60, 80	2
4	1	5	80	1, 2, 4, 6

$$R = [(m_2 - m_1) \times C]/V \quad (1)$$

where R is the preservative loaded onto the specimens (g/m^3), C is the concentration of the modified nano-Ag/TiO_2 (%), V is the volume of the specimen (m^3), m_1 is the weight of the specimen before preservative soaking (g), and m_2 is the weight of the specimen after preservative soaking (g).

Properties of fixation rate

Properties of leach-resistant tests were conducted according to American Wood Protection Association (AWPA) Standard E11-97 (AWPA 1996). Twelve specimens were treated with each specific condition shown in Table 1. To determine the weight gain percentage, all of the specimens were oven-dried and weighed (M_1), and then soaked in antimold preservative, oven-dried, and weighed again (M_2). The weight gain percentage (W_1) of the specimens was calculated as

$$W_1 = (M_2 - M_1)/M_1 \times 100\% \quad (2)$$

where M_2 is the absolute dry weight of the specimen after preservative soaking, M_1 is the absolute dry weight of the specimen before preservative soaking, and W_1 is the weight percentage gain of the specimen before leachability experiments (%).

The specimens were then soaked in distilled water with stirring. The water was replaced at 5, 10, 24, and 48 hours. After water soaking, the specimens were dried and their ovendry weights (M_3) were recorded. The weight gain percentage after leachability experiments (W_2) was calculated as

$$W_2 = (M_3 - M_1)/M_1 \times 100\% \quad (3)$$

where M_3 is the ovendry weight of the specimen after leachability experiments and W_2 is the weight gain percentage after leachability experiments (%).

The leaching rate of the specimens (P) and the fixation rate of the specimens (G) were calculated by Equations 4 and 5, respectively,

$$P = (W_1 - W_2)/W_1 \times 100\% \quad (4)$$

$$G = 1 - P \quad (5)$$

where P is the leaching rate (%) and G is the fixation rate (%).

FE-SEM, XRD, and FTIR characterization

Modified nano-Ag/TiO_2 was prepared from 1.5 wt% KH-550 and 5 wt% nano-Ag/TiO_2 and reacted at 80°C for 2 hours (Zhou 2015). The unmodified and modified nano-Ag/TiO_2, untreated and treated wood specimens were placed in a vacuum oven until oven-dried and then analyzed by FE-SEM, XRD, and FTIR. An ultra-high-resolution scanning electron microscope (SU8010 UHR) operating at an accelerating voltage of 10 kV was used to observe the morphology of the specimens to determine their surface characteristics. The crystallinity of the powder (50 mesh) from specimens was evaluated by an X-ray diffractometer (Bruker D8 Advance). The patterns were obtained within a 10° to 80° diffraction angle (2θ) interval, with a 0.02° step and a scan speed of 2°·min^{-1}. The degree of crystallinity was determined as the ratio of the intensity difference in the selected peak positions (Celikbag and Via 2016). FTIR was performed to characterize the surface chemical composition of the specimen. The samples were directly applied to the diamond crystal of the FTIR spectrometer (Termo Electron Nicolet Avatar 330), and the spectra were collected in transmittance mode by 32 scans in the range of 4,000 to 300 cm^{-1} at a resolution of 2 cm^{-1}.

Results and Discussion

Effect of KH-550 concentration on wood antimold properties

The growth of bacteria fungi on wood surfaces was mainly attributed to *Aspergillus niger*, *Trichoderma viride*, and *Penicillium citrinum* (Feng et al. 2009). As expected, it was found that, in most cases, increasing the KH-550 concentration strengthened the antimold rate, loading amount, and leach resistance of wood specimens (Fig. 1). When the concentration was 1.5 wt%, the antimold performance, loading amount, and leach resistance of wood specimens increased by 55.6, 5.6, and 12 percent more than those treated by unmodified nano-Ag/TiO_2. These improve-

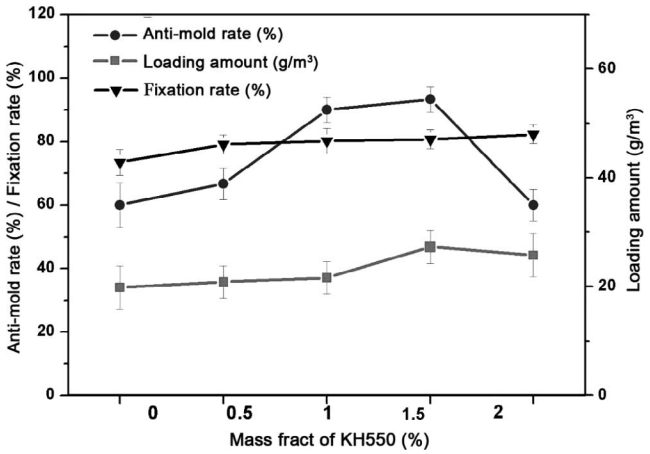

Figure 1.—Effect of KH-550 concentration on wood antimold rate, loading amount, and fixation rate (nano-Ag/TiO_2 concentration, 5 wt%; incubation time, 2 h; reaction temperature, 80°C).

ments were attributed mainly to the enhanced dispersity of the nano-Ag/TiO_2 by KH-550. The reason for the improvement may be owing to the polar nature of the nano-TiO_2 powders, which have high surface energy, resulting in aggregation within the medium or polymer matrix. However, the three ethoxy groups of KH-550 hydrolysis resulted in the formation of silanols. Dehydration condensation between the silanols and hydroxyl groups on the TiO_2 surface significantly reduced the surface hydrophilicity of the TiO_2 particles due to the decrease in hydroxyl groups; this effectively reduced the surface energy and significantly improved the dispersion of the nano-TiO_2 particles because of the electrostatic repulsion between KH-550 molecule chains (Li et al. 2008, Zhang et al. 2008). As KH-550 content increased, a greater portion of TiO_2 was modified, and smaller aggregates were formed. These factors promoted the material's photocatalytic and antimicrobial activities. When the particle size reached the nanometer scale, the particles were able to enter the lumen of wood cells or even diffuse into the cell walls or fill pores in the cell walls, and these advantages could improve the leach resistance of the TiO_2 particles (Wang et al. 2012). Once KH-550 content grew excessively, the hydrolysis of excess silane couplers produced methylsiloxane anions that attacked the Si in the silane couplers and formed cross-links between TiO_2 particles, resulting in flocculation of TiO_2 particles and thus reducing the loading amount. The diagram of grafting KH-550 on nano-TiO2 particle surface is shown in Figure 2.

Effect of nano-Ag/TiO_2 concentration on wood antimold properties

Figure 3 shows the relationship between increased nano-Ag/TiO_2 concentration and the antimold rate, loading amount, and leach resistance of wood specimens. The loading amount increased sharply as the concentration of nano-Ag/TiO_2 increased, while the specimens' antimold rate and leach resistance gradually decreased.

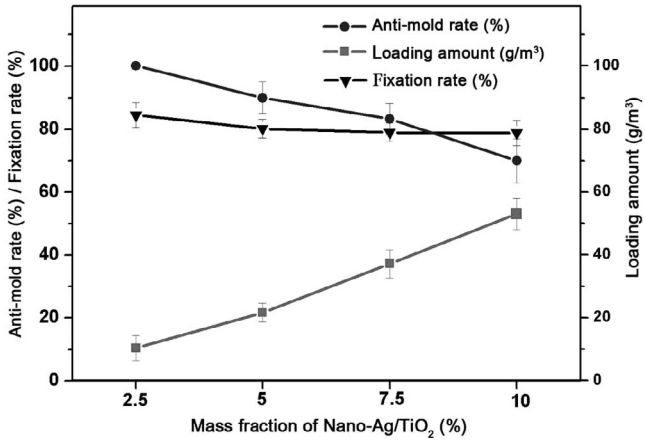

Figure 3.—Effect of nano-Ag/TiO_2 concentration on wood antimold rate, loading amount, and fixation rate (KH-550 concentration, 1 wt%; incubation time, 2 h; reaction temperature, 80°C).

When 2.5 wt% Ag/TiO_2 was applied, the specimens presented maximum antimold rate, up to 100 percent. This suggested that the distance between particles is larger in low-concentration Ag/TiO_2 solutions, thereby enhancing particle dispersivity and reducing aggregation; this allowed the Ag/TiO_2 particles to penetrate into the wood capillary structure. Additionally, when the modified nano-Ag/TiO_2 was smaller aggregates, it had stronger photocatalytic activity and produced more electron-hole pairs under light. This activated the atmospheric oxygen molecules to produce reactive oxygen species that could kill mold on the wood material surface.

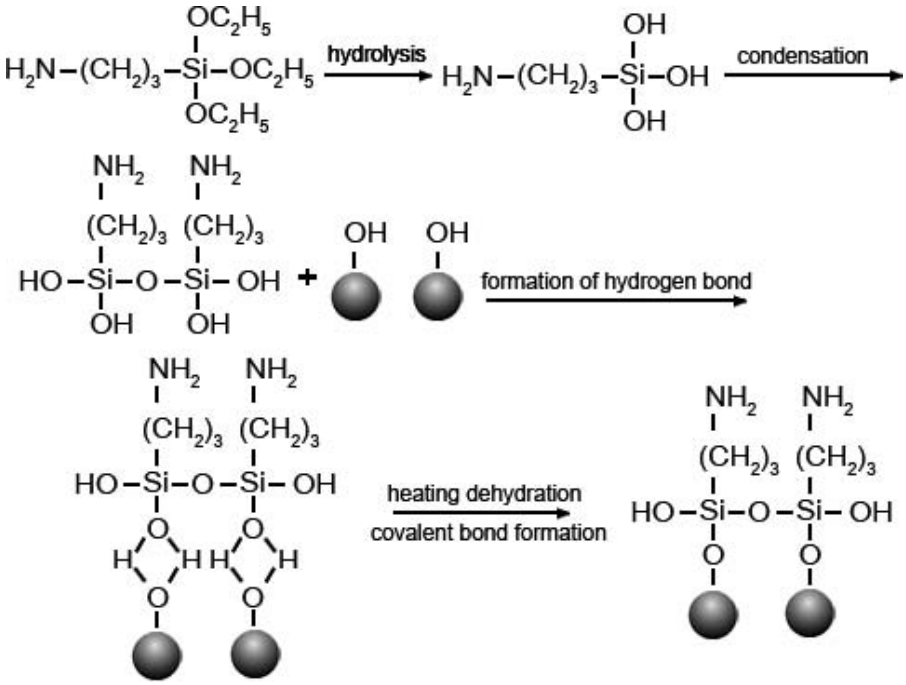

Figure 2.—Diagram of grafting KH-550 on nano-TiO_2 particle surface.

Nano-Ag/TiO_2 concentration exerted a significant effect on the loading amount. At a KH-550 concentration of 10 wt%, the loading amount was 53.01 g/m^3, and the fixation rate was the lowest, at 81.8 percent. According to a previous study, nano-Ag/TiO_2 particles attach mostly to the axial tracheid and fiber of wood, while a small fraction penetrates into wood cell lumens and attach to cell walls through chemical bonding or physical interactions (Wang 2012). However, because conifers do not have vessels, it is more likely that the nanoparticles penetrated the lumen of the tracheid given that these cells account for 90 to 95 percent of the tissue. During the soaking treatment, large amounts of nano-Ag/TiO_2 particles were retained; higher nano-Ag/TiO_2 concentrations increased the probability of collision among nano-TiO_2 particles and between the nano-Ag/TiO_2 particles and wood, thus increasing their attachment and aggregation and likewise increasing the loading amount. Aggregation contributed to the formation of particles that were too large to efficiently penetrate into the wood specimens and consequently were retained in the void spaces of the wood surface. As a result, the nano-Ag/TiO_2 vulnerability to leaching and the fixation rate decreased.

Effect of reaction temperature on wood antimold properties

It was found that increasing the reaction temperature enhanced the antimold rate, loading amount, and fixation rate of all specimens at lower temperatures, but then these metrics decreased at higher temperatures. All three indices reached optimal levels at 60°C (Fig. 4). Previous studies have shown that reaction of KH-550 and TiO_2 is an endothermic process. Higher temperatures increase the reaction speed and contribute to more thorough reactions, thus improving modification efficiency. The excessive temperature leads to excessive hydrolysis and condensation, resulting in self-condensation of KH-550 during the experiment and a reduction in the efficiency of Ag/TiO_2 modification. Furthermore, high temperatures also resulted in faster thermal motion of nano-Ag/TiO_2 particles and increased their probability of collision, contributing to the reaggregation of nanoparticles. As a result, the nano-Ag/TiO_2 particles were not able to disperse stably or evenly above 60°C.

Effect of incubation time on wood antimold properties

The effects of modified nano-Ag/TiO_2 incubated with KH-550 for different incubation periods on wood properties are shown in Figure 5. The fixation rate of nano-Ag/TiO_2 gradually increased with longer reaction time with a rapid increase in fixation rate between 0 and 4 hours. However, there was only a slight increase with an extended reaction (4 and 6 h). In the beginning, the antimold rate and loading amount rapidly increased with the extension of reaction time and then decreased after 2 hours. A 2-hour incubation time resulted in an optimal antimold rate with the highest loading amount: 90 percent and 29 g/m^3, respectively. This phenomenon was reasonable, as longer reaction duration allowed for more thorough reaction between KH-550 and nano-Ag/TiO_2. This interaction resulted in a more efficient modification and a significant increase in dispersivity. Owing to steric hindrance, the couplers could react with only a portion of the hydroxyl groups on the nano-Ag/TiO_2 surface. As a result, the reactions reached equilibrium at 2 hours. Additionally, there were physical interactions between KH-550 and nano-Ag/TiO_2 surfaces that can be divided into two stages: the monolayer adsorption formation and the micelle formation (Bourgeat-Lam et al. 1995). Upon the monolayer adsorption formation, the couplers started to form micelles that affected the loading amount and antimold rate. Excessive reaction time resulted in Ag oxidation and generated AgO, thus decreasing the antimicrobial effects of Ag and presenting a negative impact on the antimold rate of nano-Ag/TiO_2.

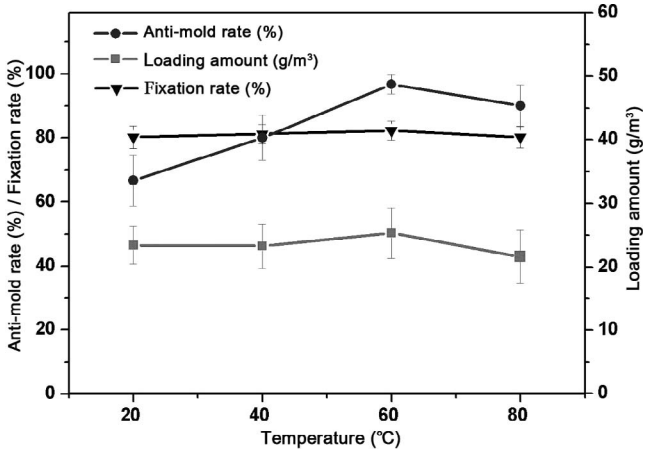

Figure 4.—Effect of reaction temperature on wood antimold rate, loading amount, and fixation rate (KH-550 concentration, 5 wt%; nano Ag/TiO_2 concentration, 1 wt%; incubation time, 2 h).

FE-SEM analysis

Radial sections (Figs. 6a, 6c, and 6d) and cross section (Fig. 6b) of Masson pine wood specimens were observed with FE-SEM to determine the dispersion of modified nano-Ag/TiO_2.

Based on Figures 6a and 6b, the modified nanoparticles impregnated in the tracheid and attached to the cell walls through chemical bonds or physical interactions (Wang 2012). According to Figures 6c and 6d, the modified nano-

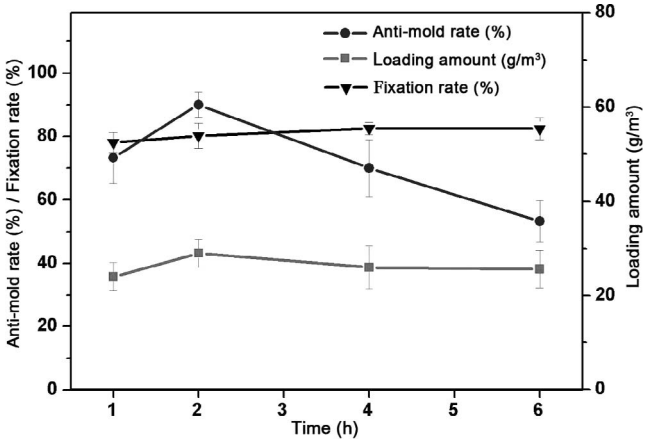

Figure 5.—Effect of incubation time on wood antimold rate, loading amount, and fixation rate (KH-550 concentration, 1 wt%; nano-Ag/TiO_2 concentration, 1 wt%; reaction temperature, 80°C).

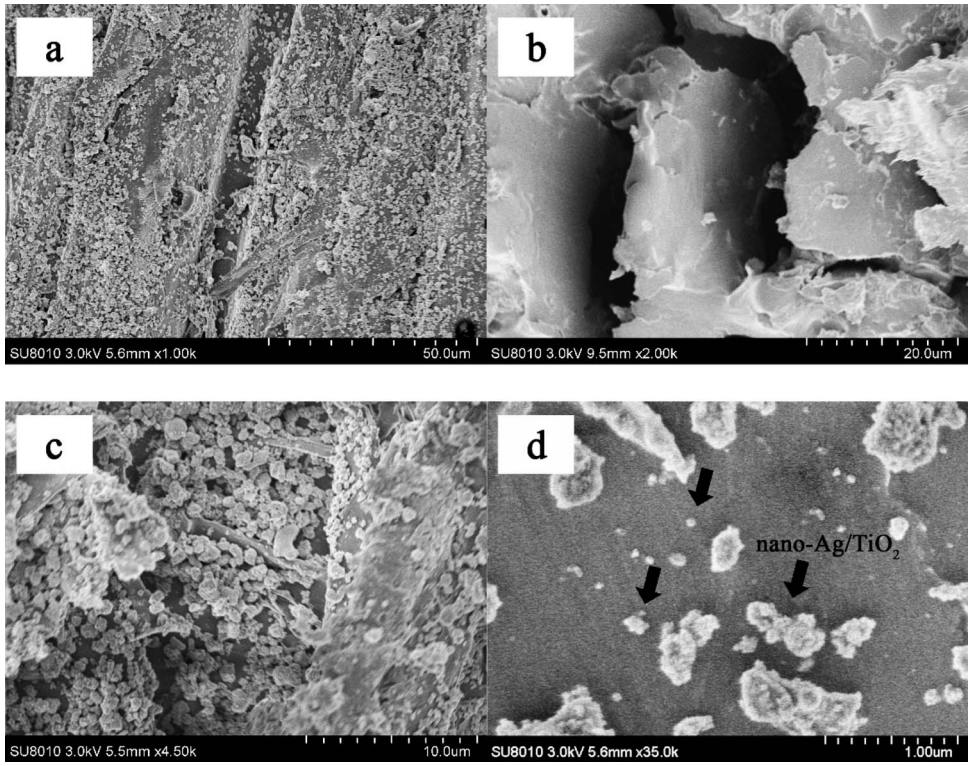

Figure 6.—Field emission scanning electron microscopy image of dispersion of modified nano-Ag/TiO_2 in Masson pine wood: radial sections (a, c, and d) and cross section (b).

Ag/TiO_2 penetrated into the wood tracheid lumen and formed tight flocculent precipitates. This is due to the hydroxyl groups resulting from coupler hydrolysis-formed hydrogen bonding with the unsaturated hydroxyl groups on the nano-Ag/TiO_2 surface, which contributed to the formation of a reticular structure that coated the nano-Ag/TiO_2 surface and thus improved the dispersion of modified nanoparticles (Zhou 2015). The modified nanoparticles presented decent dispersion, although some aggregations still exist.

XRD analysis

Figure 7 shows the XRD spectra results of nano-Ag/TiO_2 (A) and modified Ag/TiO_2 (B). In the spectrum of unmodified Ag/TiO_2, characteristic peaks of anatase TiO_2 were observed at 25.3°, 37.7°, 48.0°, 53.7°, and 62.2°, while the characteristic peaks of Ag were observed at 35.9°, 40.3°, 55.1°, and 59.1°, respectively. Comparing the two curves, the position of the diffraction peaks suggested that the elemental Ag was attached to the TiO_2 surface. A small fraction of TiO_2 presented rutile structures due to the Ag attachment. In addition, the modification did not change the aforementioned characteristics of Ag/TiO_2, suggesting that the photocatalytic activity and antimold rate of Ag/TiO_2 were retained after modification.

The XRD spectra of the untreated wood (A), nano-Ag/TiO_2–treated wood (B), and modified nano-Ag/TiO_2–treated wood (C) are shown in Figure 8. In spectrum A, obvious peaks were observed at 17°, 22.2°, 22.5°, and 35°, representing the crystalline faces (100), (002), and (040) of cellulose. The spectrum of the nano-Ag/TiO_2–treated specimen (spectrum B) retained characteristics of untreated wood (spectrum A) but exhibited lower intensity at 17°, 22.2°, and 22.5° as well as characteristic peaks of anatase TiO_2 at 25.3°, 37.7°, 48.0°, 53.7°, and 62.2° that were absent from spectrum A. These observations suggest that after penetrating into the wood specimen, the nano-Ag/TiO_2 retained characteristic structures of anatase TiO_2 and thus retained photocatalytic activity. The decreased intensity of spectrum B was due to the addition of nanoparticles having reduced the cellulose content in the specimen. A portion of the nanoparticles reached the amorphous regions of cellulose and reacted with the hydroxyl groups, increasing the total volume of cellulose and thus reducing the diffraction intensity and degree of crystallinity of the wood specimen (Wang et al. 2012). Compared with spectrum B, spectrum C presented even further reduced intensity at 17° and 22.5°; this was because the modified nano-Ag/TiO_2 had better dispersivity and smaller particle size and thus penetrated into the tracheid lumen more efficiently.

FTIR analysis

The FTIR spectra of the unmodified and modified nano-Ag/TiO_2 are shown in Figure 9. The peak at 3,422 cm^{-1} was assigned to the stretching of hydroxyl groups (-OH) on the TiO_2 surface, and the peak at 1,626 cm^{-1} resulted from the bending vibration of O-H in water molecules attached to the TiO_2. The broad band at 500 to 700 cm^{-1} represents the characteristic peak of Ti-O-Ti. Organic functions were clearly observed in the spectrum of modified nano-TiO_2, including characteristic peaks of methyl groups (-CH_3) and methylene groups (-CH_2-) at 2,925 and 2,850 cm^{-1}, respectively. Peaks representing the in-plane bending vibration of amino groups (N-H) and stretching of C-N

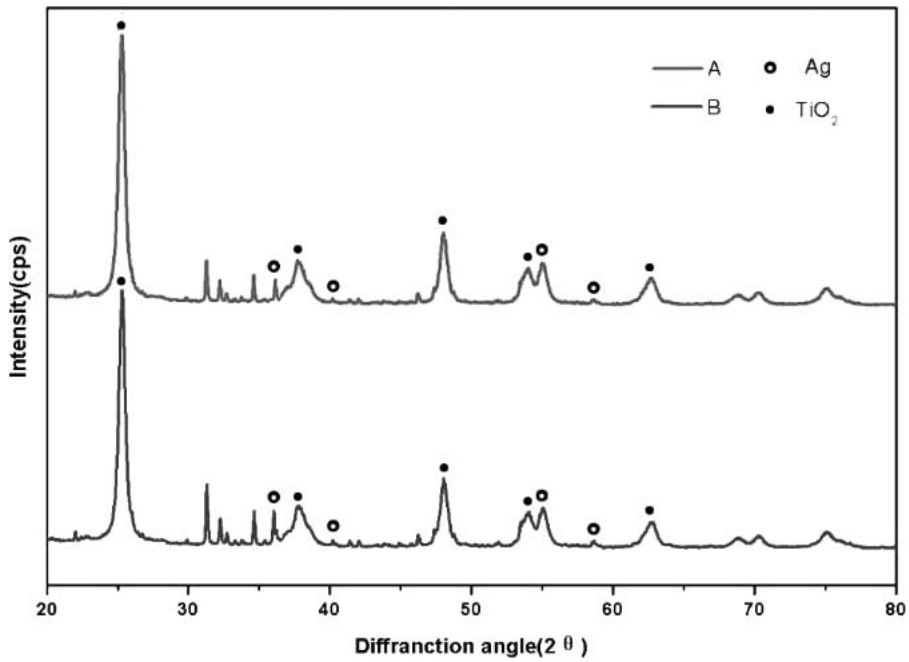

Figure 7.—X-ray diffraction spectra of unmodified (A) and modified (B) nano-Ag/TiO_2.

bonds were observed at 1,635 and 1,127 cm^{-1}, respectively. Characteristic peaks of Si-O-Ti were observed at 972 and 934 cm^{-1}. These observations altogether indicate efficient bonding effects between nano-TiO_2 and KH-550.

The FTIR spectra of the untreated wood (A), nano-Ag/TiO_2–treated wood (B), and modified nano-Ag/TiO_2–treated wood (C) are shown in Figure 10. Compared with spectrum A, spectrum B presented the characteristic peak of Ti-O-C at 610 cm^{-1} and a broad absorption band at 700 to 500 cm^{-1}, i.e., the characteristic peak of Ti-O-Ti. In addition, the peak at 3,500 to 3,000 cm^{-1} assigned to hydroxyl groups (-OH) showed reduced intensity in spectrum B, indicating the formation of hydrogen bonds between TiO_2 and hydroxyl

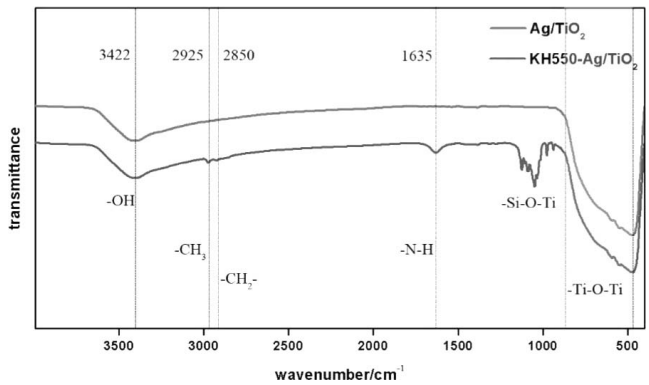

Figure 9.—Fourier transform infrared spectroscopy spectra of unmodified and modified nano-Ag/TiO_2.

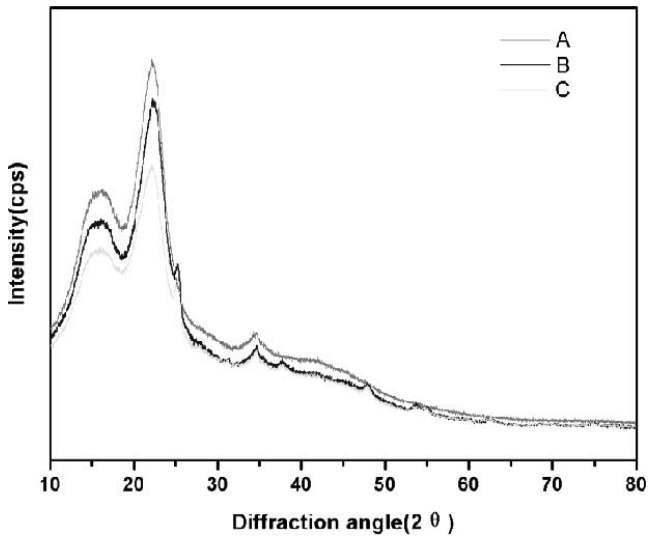

Figure 8.—X-ray diffraction spectra of untreated wood (A), nano-Ag/TiO_2–treated wood (B), and modified nano-Ag/TiO_2–treated wood (C).

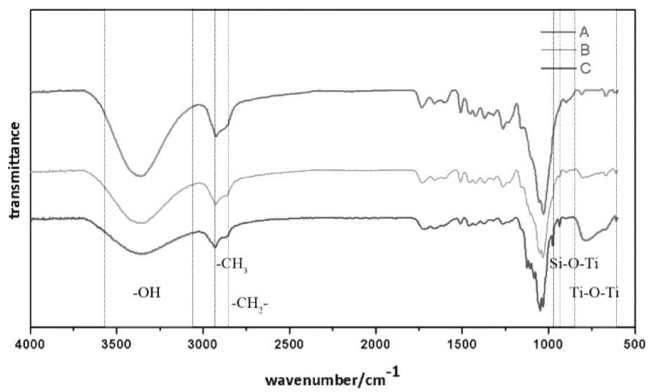

Figure 10.—Fourier transform infrared spectroscopy spectra of untreated wood (A), nano-Ag/TiO_2–treated wood (B), and modified nano-Ag/TiO_2–treated wood (C).

groups on the wood surface. In spectrum C, peaks assigned to the stretching of methyl groups (-CH_3) and methylene groups (-CH_2-) were observed at 2,890 to 2,850 cm^{-1}. The characteristic peak of Si-O-Si was observed at 1,100 to 1,000 cm^{-1}, and the characteristic peaks of Si-O-Ti were observed at 980 and 938 cm^{-1}, suggesting that modified nano-TiO_2 penetrated effectively into the wood cell walls. The peak representing Ti-O-C was observed at 610 cm^{-1}, but no Si-C–associated peak was observed, suggesting that modification did not affect the bonding between the nanoparticles and wood.

Conclusions

Modification of nano-Ag/TiO_2 by KH-550 enhanced the antimold rate, loading amount, and fixation rate of the mold-proof–treated wood. The treated wood presented optimum properties when the KH-550 concentration, nano-Ag/TiO_2 concentration, reaction temperature, and incubation time were 1.5 wt%, 2.5 wt%, 60°C, and 2 hours, respectively. The binding affinity and surface energy of nano-TiO_2 were reduced and the dispersivity of nano-Ag/TiO_2 particles improved after modification. The modified nano-Ag/TiO_2 was able to penetrate into the wood specimens and be retained in the tracheid through successful attachment to the wood cell wall due to a tight flocculent structure. Modified nano-Ag/TiO_2 efficiently cross-linked with the wood hydroxyl groups, resulting in better fixation. Modification did not affect the anatase diffraction pattern of nano-Ag/TiO_2 or its photocatalytic and antimicrobial activities.

Acknowledgments

The authors are grateful for the support of the State Bureau of Forestry 948 Project (2015-4-51), the Fundamental Research Funds for the Central Universities (2018ZY12), and supported by Beijing Natural Science Foundation (6184045).

Literature Cited

Akira, F., N. T. Tata, and A. T. Donald. 2000. Titanium dioxide photocatalysis. *J. Photochem. Photobiol. C Photochem. Rev*. 1(1):1–21.

American Wood Protection Association (AWPA). 1996. Standard method of determining the leachability of wood preservatives. Standard E11-97. AWPA, Birmingham, Alabama.

Bourgeat-Lam, E., P. H. Espiard, and A. Guyot. 1995. Poly (ethyl acrylate) latexes encapsulating nano particles of silica: 1. Functionalization and dispersion of silica. *Polymer* 36(23):4385–4389.

Celikbag, Y. and B. K. Via. 2016. Characterization of residue and bio-oil produced by liquefaction of loblolly pine at different reaction times. *Forest Prod. J*. 66(1):29–36.

China Timber Standardization Technical Committee. 2000. Testing method for anti-mould chemicals in controlling mould and blue stain fungi on wood. GB/T 18261-2000. Standardization Administration of China, Beijing.

Feng, N. C., D. Y. Xu, and W. Qiong. 2009. Antifungal capability of TiO_2 coated film on moist wood. *Building Environ*. 44(5):1088–1093.

Li, S., K. Wang, J. Cheng, and Z. Y. Li. 2008. Synthesis of TiO_2/Poly (styrene-co-divinybenzene) nanocomposite microspheres by grafting copolymerization. *Chin. J. Chem*. 26(4):781–786.

Liu, Y., H. W. Guo, J. M. Gao, F. Zhang, L. M. Shao, and B. K. Via. 2015a. Effect of bleach pretreatment on surface discoloration of dyed wood veneer exposed to artificial light irradiation. *BioResources* 10(3):5607–5619.

Liu, Y., L. M. Shao, J. M. Gao, H. W. Guo, Y. Chen, Q. Z. Cheng, and B. K. Via. 2015b. Surface photo-discoloration and degradation of dyed wood veneer exposed to different wavelength of artificial light. *Appl. Surface Sci*. 311:353–361.

Miyafuji, H. and S. Saka. 1997. Fire-resisting properties in several TiO_2 wood-inorganic composites and their topochemistry. *Wood Sci. Technol*. 31(6):449–455.

Nelson, K. and Y. Deng. 2008. Effect of polycrystalline structure of TiO_2 particles on the light scattering efficiency. *J. Colloid Interface Sci*. 319(1):130–139.

Rengaraj, S. and X. Z. Li. 2006. Enhanced photocatalytic activity of TiO_2 by doping with Ag for degradation of 2,4,6-trichlorophenol in aqueous suspension. *J. Mol. Catal. A Chem*. 243(1):60–67.

Rincón, A.-G. and C. Pulgarin. 2004. Bactericidal action of illuminated TiO_2 on pure *Escherichia coli* and natural bacterial consortia: Post-irradiation events in the dark and assessment of the effective disinfection time. *Appl. Catal. B Environ*. 49(2):99–112.

Sun, Q. F. 2012. Controlled fabrication and properties of inorganic nanomaterials grown onto the wood surface using a low-temperature-cosolvent hydrothermal method. Master's thesis. Northeast Forestry University, Heilongjiang, China.

Sun, Q. F., H. P. Yu, Y. X. Liu, J. Li, Y. Z. Cui, and Y. Liu. 2010. Prolonging the combustion duration of wood by TiO_2 coating synthesized using cosolvent-controlled hydrothermal method. *Mater. Sci*. 45(24):6661–6667.

Wang, M. 2012. Study on preparation and fixation mechanism of nano-TiO_2 based wood preservative. Master's thesis. Central South University of Forestry and Technology, Hunan, China.

Wang, X. F., R. Yu, K. Wang, G. Q. Yang, and H. G. Yu. 2015. Facile template-induced synthesis of Ag-modified TiO_2 hollow octahedra with high photocatalytic activity. *Chin. J. Catal*. 36(12):1211–2218.

Wang, X. Q., J. L. Liu, and Y. B. Chai. 2012. Thermal, mechanical and moisture absorption properties of wood-TiO_2 composites prepared by a sol-gel process. *BioResources* 7(1):893–901.

Xue, C. H., S. T. Jia, H. Z. Chen, and M. Wang. 2008. Super hydrophobic cotton fabrics prepared by sol-gel coating of TiO_2 and surface hydrophobization. *Sci. Technol. Adv. Mater*. 9(3):035001. DOI:10.1088/1468-6996/9/3/035001

Ye, J. H. 2006. Research on slice modified by nano-TiO_2. Master's thesis. Fujian Agriculture and Forestry University, Fujian, China.

Zhang, X. D., H. J. Su, Y. Zhao, and T. Tan. 2008. Antimicrobial activities of hydrophilic polyurethane/titanium dioxide complex film under visible light irradiation. *J. Photochem. Photobiol. A Chem*. 199(2):123–129.

Zhou, L. 2015. Study on preparation technology and properties of board decorated by antimicrobial impregnated veneer. Master's thesis. Beijing Forestry University, Beijing, China.